



PAPER

A mechanistic relative biological effectiveness model-based biological dose optimization for charged particle radiobiology studies

RECEIVED
14 August 2018REVISED
9 November 2018ACCEPTED FOR PUBLICATION
4 December 2018PUBLISHED
21 December 2018Fada Guan^{1,6}, Changran Geng², David J Carlson³, Duo H Ma¹, Lawrence Bronk⁴, Drake Gates⁵, Xiaochun Wang¹, Stephen F Kry¹, David Grosshans⁴ and Radhe Mohan¹¹ Department of Radiation Physics, The University of Texas MD Anderson Cancer Center, Houston, TX 77030, United States of America² Department of Nuclear Science and Engineering, Nanjing University of Aeronautics and Astronautics, Nanjing 210016, People's Republic of China³ Department of Therapeutic Radiology, Yale University School of Medicine, New Haven, CT 06511, United States of America⁴ Department of Radiation Oncology, The University of Texas MD Anderson Cancer Center, Houston, TX 77030, United States of America⁵ Orbital Debris Program Office, NASA Johnson Space Center, Houston, TX 77058, United States of America⁶ Author to whom any correspondence should be addressed.E-mail: FGuan@mdanderson.org**Keywords:** charged particle, RBE, Monte Carlo, python, biological dose optimization, RMFSupplementary material for this article is available [online](#)

Abstract

In charged particle therapy, the objective is to exploit both the physical and radiobiological advantages of charged particles to improve the therapeutic index. Use of the beam scanning technique provides the flexibility to implement biological dose optimized intensity-modulated ion therapy (IMIT). An easy-to-implement algorithm was developed in the current study to rapidly generate a uniform biological dose distribution, namely the product of physical dose and the relative biological effectiveness (RBE), within the target volume using scanned ion beams for charged particle radiobiological studies. Protons, helium ions and carbon ions were selected to demonstrate the feasibility and flexibility of our method. The general-purpose Monte Carlo simulation toolkit Geant4 was used for particle tracking and generation of physical and radiobiological data needed for later dose optimizations. The dose optimization algorithm was developed using the Python (version 3) programming language. A constant RBE-weighted dose (RWD) spread-out Bragg peak (SOBP) in a water phantom was selected as the desired target dose distribution to demonstrate the applicability of the optimization algorithm. The mechanistic repair-misrepair-fixation (RMF) model was incorporated into the Monte Carlo particle tracking to generate radiobiological parameters and was used to predict the RBE of cell survival in the iterative process of the biological dose optimization for the three selected ions. The post-optimization generated beam delivery strategy can be used in radiation biology experiments to obtain radiobiological data to further validate and improve the accuracy of the RBE model. This biological dose optimization algorithm developed for radiobiology studies could potentially be extended to implement biologically optimized IMIT plans for patients.

1. Introduction

Charged particle therapy⁷, such as proton and heavy ion therapy, has become much more common in recent years worldwide, partly because clinical trials have shown promising results (Eaton *et al* 2016, Yock *et al* 2016). In addition, economic factors and the development of more advanced technology (e.g. compact treatment facility designs) have led to increased use of particle therapy (Flanz and Bortfeld 2013, Mailhot Vega *et al* 2013). As the

⁷Terms 'charged particle therapy', 'particle therapy' and 'ion therapy' are used interchangeably in this article.

cost of particle therapies continues to drop, the number of centers is predicted to increase dramatically. Despite the physical and clinical advantages in treating some disease sites, many challenges still exist for the radiobiology of particle therapy. This also means many opportunities are available to further investigate the biological characteristics of particle therapy (Jones *et al* 2018, Paganetti 2018).

The standard beam delivery technique for particle therapy is now transitioning to more advanced beam scanning technology. Nearly all of the newly built or planned particle therapy centers are equipped with scanning nozzles (Particle Therapy Co-Operative Group 2017). This development allows for the use of intensity-modulated ion therapy (IMIT) by optimizing the weight of each constituent particle beamlet to deliver the desired dose to the target tumor. For proton therapy, IMPT is specifically referred to as intensity-modulated proton therapy. IMIT may provide the potential to both reduce normal tissue exposure and enhance biological effects in target tumor volumes by placing more 'biologically effective' particles into the target while preferentially sparing critical organs. In biologically optimized IMIT ('bio-IMIT') plans, an isometric therapeutic effect is expected to occur in the target tumors. The generation of bio-IMIT plans requires appropriate biophysical models to calculate the RBE of particles at different locations. A plan optimizer is required to integrate the detailed biological characteristics of each beamlet into the optimization process to find the optimal solution for the weight of each beamlet. Although bio-IMIT may provide a great potential to improve the therapeutic index of particle therapy, the use of different biophysical models in treatment planning can predict different biological effects (Gillmann *et al* 2018).

The descriptions of some typical RBE models can be found in previous studies (Hawkins 1994, 1996, Scholz *et al* 1997, Wilkens and Oelfke 2004, Tilly *et al* 2005, Carabe-Fernandez *et al* 2007, Elsässer and Scholz 2007, Kase *et al* 2007, Elsässer *et al* 2008, 2010, Chen and Ahmad 2011, Frese *et al* 2012, Wedenberg *et al* 2013, Carlson *et al* 2008, Kamp *et al* 2015, McNamara *et al* 2015). In general, these models can be divided into two main categories: phenomenological and mechanistic. In a phenomenological RBE model, α and β coefficients of the linear-quadratic (LQ) relationship derived from cell survival curves can be expressed as a function of physical quantities, i.e. LET or lineal energy, with some empirical or semi-empirical coefficients usually derived from experimental data (Wilkens and Oelfke 2004). A phenomenological model is usually limited to protons only. In a mechanistic RBE model, the underlying interaction mechanisms between ionizing radiation and the target cells, e.g. particle track structures, and DNA damage and repair, are usually involved in the modeling process (Kase *et al* 2007, Frese *et al* 2012). A mechanistic model usually can be applied to any radiation type. Some typical mechanistic RBE models include the repair-misrepair-fixation (RMF) model (Carlson *et al* 2008, Frese *et al* 2012, Kamp *et al* 2015), the microdosimetric-kinetic model (MKM) (Hawkins 1996, 1998), and the local effect model (LEM) (Elsässer *et al* 2010). These three models and their underlying biological mechanisms have been recently reviewed and compared by Stewart *et al* (2018). In addition to the development of RBE models, mathematical models have been developed to assess the tumor and normal tissue responses (Jones 1999). Furthermore, the RBE effects have been assessed using the concept of biologically effective dose (Dale and Jones 1999).

The RBE value of protons relative to photons currently used in the clinic is assumed to be 1.1 regardless of proton beam characteristics, depth in tissue, dose, dose rate, and target cell types (Paganetti *et al* 2002, ICRU 2007, Paganetti 2014). This is likely to be the case in the middle of the spread-out Bragg peak (SOBP). In regions proximal to the SOBP midpoint, RBE is likely to be less than 1.1 and may in fact lead to underdosing of the tumor (Frese *et al* 2012, Jones 2014). Proton RBE at greater depths, particularly at points near, at, and beyond the distal edge, may be considerably higher (Mohan *et al* 2017). Because the distal edge in proton therapy is often within normal tissues in the distal margins, and will receive the full dose from the field, the biological effect can be significant depending on the type of tissue (Jones 2014). In addition, this generic proton RBE has been challenged by recent experimental data using scanned proton beams, which have revealed the spatial variation in biological effects along the Bragg curve, with a sharp increase of RBE at the Bragg peak and within the distal edge (Britten *et al* 2013, Chaudhary *et al* 2014, Guan *et al* 2015a, Howard *et al* 2017). Unlike proton therapy, no generic RBE values have been applied for helium and carbon ions due to their prominent spatial variation of RBE. For carbon ion therapy, the LEM and modified-MKM models have been incorporated in clinical treatment planning systems (TPS) in Europe and Japan, respectively, to construct bio-IMIT treatment plans (Krämer *et al* 2000, Krämer and Scholz 2000, Inaniwa *et al* 2010, Stock *et al* 2015). The RMF model has been integrated into the research build of the RayStation (RaySearch Laboratories AB, Stockholm, Sweden) TPS. The RMF model is also available in a number of research-oriented TPS (Kamp *et al* 2015, 2017, Polster *et al* 2015, Qin *et al* 2018). For example, in a recent preclinical study, Qin *et al* incorporated the RMF model into a TPS for performing the biological dose optimization for carbon ion therapy (Qin *et al* 2018).

Biological dose optimization is more complicated to implement than standard optimization schemes because the biological dose from different beamlets cannot be simply summed in a linear way as is the case with physical dose. Furthermore, for ions such as helium and carbon, the heterogeneity of the biological effects from primary and secondary particles in a mixed radiation field adds additional complexities (Kramer and Scholz 2000, Hara *et al* 2012, Sakama *et al* 2012). Our team has previously developed a biological dose optimization algorithm for

scanned proton beams involving the phenomenological McNamara RBE model (McNamara *et al* 2015, Guan *et al* 2018). In the current study, our biological dose optimization algorithm was extended to heavier ions. The purpose was to develop a generic and easy-to-implement method to generate biological dose delivery beam scan patterns to be used in future radiobiology studies. To meet the requirements of ‘generic’ and ‘efficient’ characteristics, the mechanistic RMF model was selected. The RBE predictions using the RMF model have been successfully implemented for protons (Frese *et al* 2012), helium ions (Mairani *et al* 2016), and carbon ions (Frese *et al* 2012, Kamp *et al* 2015, 2017). Furthermore, the application methods of the RMF model are straightforward and open to the particle therapy community. Different from some previous studies using the RMF model in an analytical manner, in the current study, the RMF mechanism was fully implemented in the Monte Carlo particle tracking to generate the spatial distributions of radiobiological parameters. The methodology developed in the current study can inform the design of beam delivery strategies to perform *in vitro* radiation biology experiments using the high-throughput method previously developed by our team (Guan *et al* 2015a, Patel *et al* 2017) and *in vivo* studies to investigate the beam quality dependence of RBE using animal models.

2. Material and methods

In the current study, the mechanism-based RMF model and three different types of ions—protons, helium ions and carbon ions were selected, to demonstrate the feasibility of our method for using an RBE model in the biological dose optimization algorithm. There are two steps to generate an RMF model based RBE-weighted dose distribution: (1) perform Monte Carlo simulations to generate the spatial distributions of the needed physical and radiobiological parameters by involving the RMF mechanisms in the particle tracking processes; and (2) perform the biological dose optimizations by invoking the RMF model in the iteration process to predict RBE with the Monte Carlo generated datasets as the basic input.

2.1. Basic settings in Monte Carlo simulations

The general-purpose Monte Carlo toolkit Geant4 (version 10.4) (Agostinelli 2003, Allison *et al* 2016) was used to perform the particle tracking that subsequently generated the physical and radiobiological quantities used for dose optimizations and RBE modeling. Many different typical physics lists such as ‘QBBC’, ‘QGSP_BERT’, ‘QGSP_BIC’ and ‘FTFP_BERT’ can be applied in particle therapy simulations which all provide electromagnetic and hadronic physics processes. The dose difference was found below 1% for particles within the therapeutic energy ranges using these physics lists (Geng *et al* 2018, Guan *et al* 2018). In this study, the ‘FTFP_BERT’ physics list was used as a representative. The general particle source (GPS) method was used to define the ion beams traveling along the central z axis to enter the target geometry. An $80 \times 80 \times 40 \text{ cm}^3$ water phantom was built as the target for scoring quantities of interest for different ion beams. A scoring cylinder with a radius of 40 cm and thickness of 0.01 cm was built to cover the large size of the beam spot and to maximally capture the laterally scattered particles to subsequently score the so-called integral depth dose (IDD). The production cut of secondary particles (photons, electrons, positrons, protons and all recoil ions) was set to 0.01 cm to match the smallest length (thickness in this case) of the virtual detector, which followed the recommendation made by the Geant4 collaboration (Agostinelli 2003, Allison *et al* 2016). A derivative class of Geant4’s primitive scorer was created to score the quantities of interest for each tracking step processed in the *ProcessHits()* function of the scorer by filling one-dimensional (1D) ROOT histograms (Brun and Rademakers 1997). In the current work, the abscissa of a 1D ROOT histogram is the depth in water and the ordinate can be dose, radiobiological parameters, or DNA damage yield.

For proton beams, 94 groups of energies that are used at The University of Texas MD Anderson Cancer Center Proton Therapy Center, ranging from 72.5 to 221.8 MeV with the penetration ranges (depths with 90% of peak dose in the distal falloff) of 4.0 to 30.6 cm in water, were selected for Monte Carlo simulations and dose optimizations. For ^4He ions, the energy and range data were obtained using the National Institute of Standards and Technology ASTAR database (Berger 1995). A total of 161 groups of energies, ranging from 70 to 230 MeV/u with ranges of 4.1 to 33.1 cm in water, were selected. For ^{12}C ions, the energy and range data were obtained from the Errata and Addenda: ICRU Report 73 (Sigmund *et al* 2009). A total of 161 groups of energies, ranging from 120 to 440 MeV/u with ranges of 3.6 to 32.0 cm in water, were selected. A double-layer ripple filter was modeled for carbon ions to broaden the Bragg peak. A total of 10^7 source particle histories were simulated for each beamlet to make the simulation results, e.g. total dose, meet the statistical uncertainty requirement (relative error of the mean value $<1\%$) when the dose is larger than 5% of the peak dose.

2.2. Incorporating the RMF model in Monte Carlo simulations to generate radiobiological parameters

In the mechanistic RMF model, reproductive cell death by mitotic catastrophe, apoptosis, or other cell death modes is explicitly linked to DNA double-strand break (DSB) induction and processing (Carlson *et al* 2008, Stewart *et al* 2018). An independent Monte Carlo Damage Simulation (MCDS, version 3.10A) (Stewart *et al* 2011)

can be used to simulate ion- and energy-dependent DSB yields as input for the RMF model, although other Monte Carlo models (Nikjoo *et al* 1994, 1999, Friedland *et al* 1998, 2003, Alloni *et al* 2013) or experimental measurements could also potentially be used to generate input DSB yields. In the current study, the RMF model was applied to predict the biological effects of different ion beams considering all of the contributions from primary particles and their secondary particles.

Clonogenic cell survival was selected as the primary endpoint for calculating the RBE. Non-small cell lung cancer (NSCLC) H460 cells were selected as the target cells. Gamma rays from a ^{137}Cs source were selected as the reference photons. The reference LQ parameters α_x and β_x are derived in our previous study (Guan *et al* 2015a) from cell survival data of H460 cells irradiated with ^{137}Cs photons and are used as the reference radiosensitivity parameters for RBE calculations in the current study.

The details of the RMF model and its application to calculating particle RBE can be found in Carlson *et al* (2008), Frese *et al* (2012) and Kamp *et al* (2015), and references therein. Here only some key steps are listed in applying the RMF mechanisms in Monte Carlo physics simulations to generate the spatial distributions of the radiobiological parameters needed for the next-step biological dose optimization.

- (1) Estimating the cell-specific model constants κ and θ using the physical and biophysical parameters for the specified cell type with the reference photons.
- (2) Calculating radiosensitivity parameters α_i and β_i for a charged particle (with the index i) of a given energy during the Monte Carlo particle tracking process.
- (3) Calculating dose-averaged radiosensitivity parameters α_D and β_D for a mixed field of radiation at a given spatial location (with the dose D).

The detailed calculation methods are described in the supplementary material (stacks.iop.org/PMB/64/015008/mmedia). After the Monte Carlo simulation, the spatial distributions of dose, DSB yield, α_D , and β_D in the water phantom for each beamlet can be obtained. In the current study, each of the above quantities is scored in an individual 1D ROOT histogram along the z axis of the phantom respectively. With these datasets, the RBE at different locations from a radiation field composed of multiple beamlets can be calculated.

2.3. RBE-weighted dose optimization algorithm

The Python (version 3.4.3) programming language was used to develop the biological dose optimization algorithms using the NumPy and SciPy libraries. The purpose of biological dose optimization is to deliver a specified uniform RBE-weighted dose to the target region, which means that both the physical dose and the RBE should be considered. However, RBE is also a function of the physical dose and other physical and biological factors. Therefore, RBE-weighted dose optimization is usually a dynamic and complex calculation process involving multiple iterations until the predefined objective function is minimized. The developed Python code can be used to implement three functions:

- (1) Solving beam weights and calculating the RBE in an iterative process.
- (2) Predicting cell surviving fraction using the LQ cell survival model.
- (3) Predicting the DSB yield.

The details of the optimization algorithm and the calculation process of biological effect are described in the supplementary material.

3. Results and discussion

Theoretically, any shape of the target dose distribution can be specified in the optimization process, but the optimizer may not always find appropriate solutions for the beam weights in all cases. Below only results from simple cases are shown with a uniform biological dose distribution (a flat bio-SOBP) within the target from a single direction irradiation field formed by multiple beams to demonstrate the feasibility and flexibility of our method.

The physical dose optimizations for different particles using a clinically relevant dose of 2 Gy have been reported in our previous study (Geng *et al* 2018). In the current study, the biological dose optimizations have been performed setting the target RBE-weighted dose level to be 3.80 Gy (RBE) within the SOBPs (5–10 cm) for all the three selected charged particle types. This biological dose level is the reference photon dose to cause the cell surviving fraction to be 10% for the H460 cell line in our previous study using the ^{137}Cs gamma-ray source (Guan *et al* 2015a).

After optimization, the generated biologically optimized beam delivery strategy can be used in particle radiobiology experiments to verify the accuracy of the RBE model prediction. If the model prediction is sufficiently

accurate, the cell samples at different locations across the flat biological dose SOBP are expected to have identical cell survival within the specified confidence interval, e.g. 95%.

3.1. Flat biological dose SOBP of protons

The biological dose optimization results for proton beams are shown in figure 1 as different subplots. In addition to the physical and biological dose distributions, figure 1(A) shows the spatial variation of RBE; figure 1(B) shows the dose-averaged α and β values; figure 1(C) shows the induced DSB including dose-normalized values in DSB/Gy/Gbp and absolute values in DSB/Gbp at the current dose level for each location; figure 1(D) shows the predicted cell survival.

In figure 1(A), from the entrance to the proximal rise of the SOBP, the RBE shows a slightly decreasing trend from 1.12 to 1.10. This observation can be explained using equation (16) in the supplementary material. In figure 1(B), the dose-averaged α and β values are approximately constant; therefore, with all other parameters fixed in equation (16), RBE decreases with an increase in dose, which is the dose variation trend from the entrance to the proximal edge of the SOBP. Then, the RBE increases to 1.25 until the end of the SOBP and sharply increases at the distal edge to a maximum value of 1.72 (at the depth of 10.42 cm). In figure 1(B), the dose-averaged α and β values increase slightly within the SOBP but increase sharply at the end of the range. According to the equation (16), RBE increases with the increase of dose-averaged α and β values when other parameters are fixed. The RBE values and the variation trend in the current work are consistent with the original data reported by Frese *et al* using an analytical method (Frese *et al* 2012).

After the penetration range, the physical dose from proton beams is negligible. Therefore, it is not necessary to report the RBE values. It should be noted that the reported RBE at each location is calculated at its corresponding dose level, rather than at the identical cell survival rate everywhere. Therefore, these RBE values should not simply be compared because only at identical surviving fractions will the comparison of RBE with different beam qualities be indicative of the RBE for cell survival. Nevertheless, these reported RBE values can still be used in a qualitative way to show the increasing trend of RBE along the beam path.

The RMF model directly models underlying biological mechanisms such as DSB induction and processing to predict the RBE for cell survival, rather than relying on empirical relationships between experimental data and LET_d , for example, as done in some other phenomenological RBE models (Wilkins and Oelfke 2004, McNamara *et al* 2015, Polster *et al* 2015). The depth profile of DSB yield is also generated using equation (20) in the supplementary material. In figure 1(C), the dose-normalized DSB yield is shown to vary slowly along the beam path but increases sharply at the end of the SOBP and in the dose distal edge, which actually behaves similarly to the variation trend of LET_d (Paganetti 2014, Guan *et al* 2015b). This variation trend is consistent with the observations in our previous study using the γ H2AX foci staining at the end of the range of a pristine proton beam (Guan *et al* 2015a).

In figure 1(D), the predicted surviving fraction within the SOBP is 0.1 as expected. The optimization results have thus provided a useful beam delivery strategy to investigate the biological effects along the SOBP formed by scanned beams. For example, an irradiation device can be designed to place the 12 columns of a 96-well cell culture plate at different locations so that the spatial variation of the biological effect along the SOBP can be sampled in a single irradiation run. The ten middle columns of the 96-well plate (12 columns \times 8 rows) can be placed within the SOBP, the first column proximal and the last column distal to the SOBP, as marked in figure 1(D), to investigate biological effects both inside and outside of the target region. The principle of this experimental design using the high-throughput strategy to rapidly obtain radiobiological data has been described in our previous studies (Guan *et al* 2015a, Geng *et al* 2018).

Figure 1(E) shows the beam compositions used to form the proton SOBP. 36 groups of beam energies from 81.4 MeV (range = 5 cm) to 118.6 MeV (range = 10.1 cm) were used but the data from the 81.4 MeV beam are unseen owing to their relatively low contribution. In figure 1(F), the relative difference (calculated using equation (18) in the supplementary material) between the delivered biological dose after optimization and the prescribed value varies from -1.0% to 0.7% for the whole target region but except for the target boundaries the relative difference is much lower and nearly within $\pm 0.3\%$, showing the high accuracy of the biological dose optimization.

In figures 1(B) and (C), the dose averaged α and β values, as well as the DSB yield beyond the dose distal edge, have non-zero values with large data fluctuations. They are actually the corresponding contributions from secondary particles. The dose compositions from different particle species can be analyzed to interpret these non-zero values beyond the distal edge of depth dose profile. In figure 2, the Geant4 calculated dose contributions from different species of a high-energy (207 MeV) proton beam are plotted. Beyond the dose distal falloff, the main dose contributors are secondary neutrons (essentially their recoil protons). The dose is at approximately 0.1% of the peak dose, which is negligible. These low-fluence recoil protons can result in large uncertainties of the calculated α and β values and DSB yield. Because the energy of the recoil protons is relatively low, their high-LET characteristics can result in large α and β values and DSB yield. However, it should be noted that these high

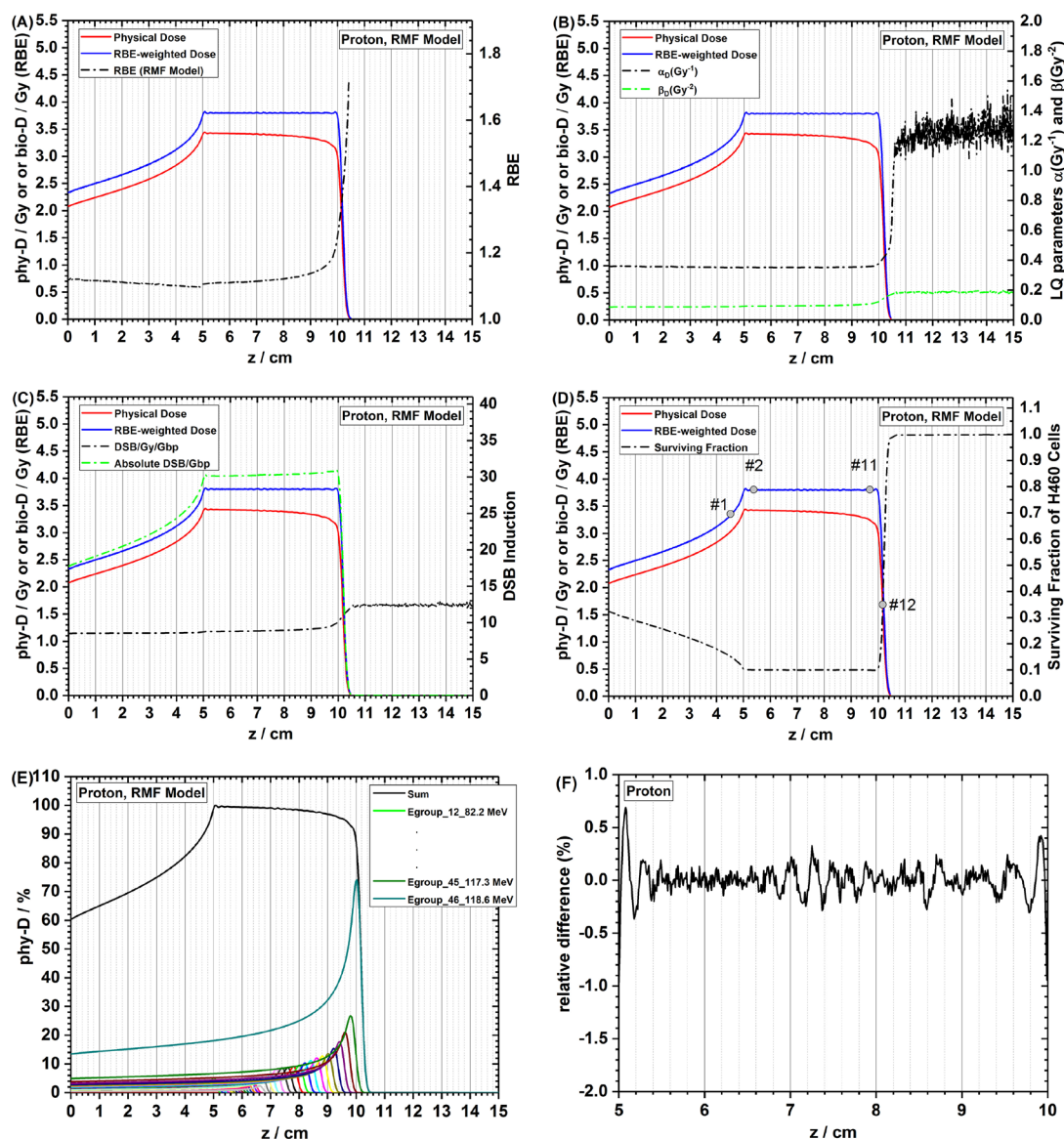


Figure 1. Biological dose optimization results of proton beams. The target region is 5 to 10 cm in water. The prescribed bio-dose value is set as 3.8 Gy (RBE). RBE and additional radiobiological parameters are calculated using the RMF model. Cell survival is calculated using the LQ model. In addition to physical dose and biological dose depth profiles, the following are shown: (A) RBE, (B) dose-averaged α and β values, (C) the DSB induction with units of DSB/Gy/Gbp and DSB/Gbp at current physical dose level and (D) the surviving fraction of H460 cells. (E) Total physical dose (%) and its constituent weighted dose components. (F) The relative difference between the delivered biological dose after the optimization and the prescribed biological dose within the target prior to the optimization.

α and β values and DSB yield do not indicate the absolute biological effect is high because the absolute dose level is negligible therein.

3.2. Flat biological dose SOBP of ^4He ions

In addition to the physical dose and biological dose, RBE, α and β , DSB yield, and cell survival of H460 cells from ^4He ions with an SOBP ranging from 5 to 10 cm in water are shown in figures 3(A)–(D). The dose fragmentation tail beyond the SOBP is clearly evident. The mixed radiation field makes a quantitative description of the biological effect of heavier ion beams more complicated. In figure 3(A), RBE for ^4He beams is higher than for proton beams. Proximal to the SOBP, the RBE varies slowly and approximately maintains a value of 1.2. Within the SOBP, the RBE increases from 1.3 to 1.8. In the distal edge, the RBE increases up to 2.3 and then decreases. In the fragmentation tail, the RBE continues to increase with the depth. The spatial variation trend of RBE values in figure 3(A) is consistent with the published data by Mairani *et al* (2016), while the numerical values are different because different target RWD values and different cell lines were used in these two studies.

The above observations can be explained using dose and LQ parameters α and β as in equation (16) in the supplementary material, from which it is apparent that RBE is a monotonically decreasing function of dose

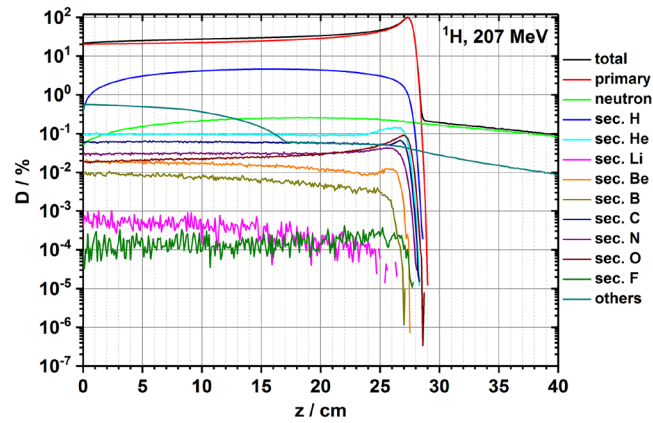


Figure 2. Percent dose contributions from primary and secondary particles for a 207 MeV proton beam in water.

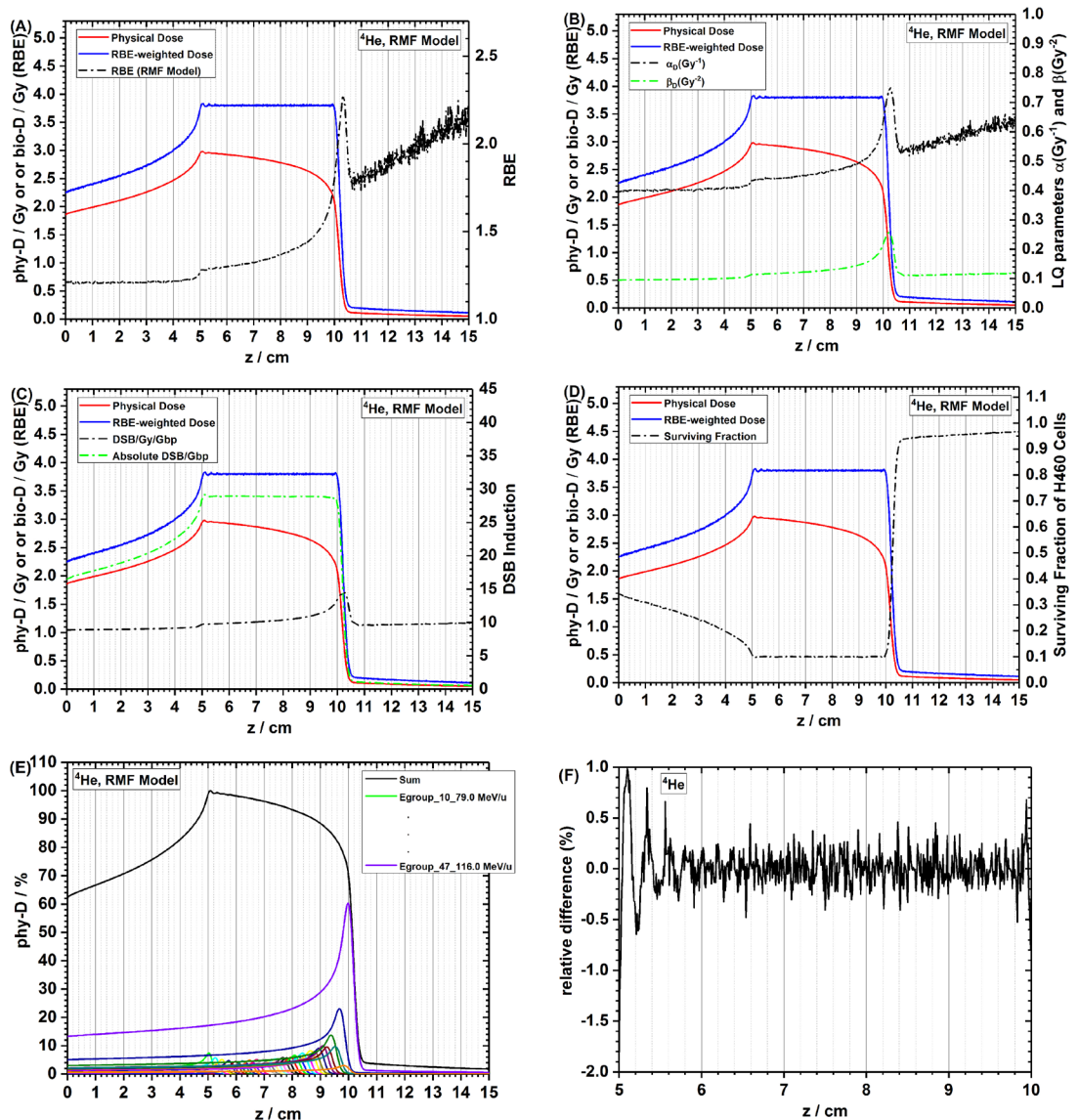


Figure 3. Biological dose optimization results of ^4He ion beams. The target region is 5 to 10 cm in water. The target biological dose value is set as 3.8 Gy (RBE). RBE and additional radiobiological parameters are calculated using the RMF model. Cell survival is calculated using the LQ model. In addition to physical dose (phy-D) and biological dose (bio-D) depth profiles, the following are shown: (A) RBE, (B) the dose-averaged α and β values, (C) the DSB induction with units of DSB/Gy/Gbp and DSB/Gbp at current physical dose level, (D) the surviving fraction of H460 cells. (E) Total physical dose (%) and its constituent weighted dose components. (F) The relative difference between the delivered biological dose after the optimization and the prescribed biological dose within the target prior to the optimization.

but an increasing function of both α and β for the specific ion if all other parameters are fixed. As shown in figure 3(B), both α and β increase in the fragmentation tail but the dose continues to drop. Therefore, an increase in the RBE in the fragmentation tail is evident. Large fluctuations are evident for RBE and α in the fragmentation tail owing to the low particle fluence, but these fluctuations do not occur for other quantities of interest. It should be noted that the increased α and β values in the fragmentation tail are caused by the decrease in energy (increase in LET) of nuclear fragments along the penetration depth. The experimental data of Furusawa *et al* have demonstrated the varying trend of α and β with LET: they first increase and then decrease (Furusawa *et al* 2000). The values predicted using the RMF model are consistent with the gathered experimental data (Frese *et al* 2012) when LET is lower than 150–200 keV μm^{-1} . Independent investigations are underway to account for the spatial proximity and complexity of individual DSBs generated by low-energy ions in the MCDS model to account for the correction for an ‘overkill’ or ‘proximity’ effect at high $(Z_{\text{eff}}/\beta)^2$ values (Butkus *et al* 2018). For the DSB induction data in figure 3(C), the normalized DSB yield (per Gy per Gbp) increases within the SOBP, but the absolute DSB yield (per Gbp) at the given dose level is unchanged across the SOBP.

The cell survival curve for ^4He ions is shown in figure 3(D). It is similar to the result obtained by using protons, except that beyond the SOBP, the surviving fraction is not 1.0 because of the non-zero dose in the fragmentation tail of ^4He ions.

Figure 3(E) shows the beam compositions used to form the ^4He SOBP. 39 groups of beam energies ranging from 78.0 to 116.0 MeV/u were used but the data from group #9 with 78.0 MeV/u and group #46 with 115.0 MeV/u are unseen owing to their relatively low contributions. In figure 3(F), the relative difference between the delivered biological dose after the optimization and the prescribed value varies from -2.0% to 1.0% for the whole target region. However, except at the target boundaries, the relative difference is much lower and nearly within $\pm 0.3\%$, showing the high accuracy of the biological dose optimization.

To interpret the observations in the fragmentation tail, a 206 MeV/u ^4He ion beam was selected as the representative to analyze the effects; specifically, the dose contributions from primary and different secondary particles were examined using Geant4. Our results, shown in figure 4, reveal that the tail’s main constituents are species with $Z = 1$, and more specifically, by secondary protons and deuterons (details not shown). The dose fragmentation tail is one of the major concerns for using ions heavier than protons because this tail can deliver unnecessary dose to surrounding normal tissues. Our simulation results also reveal that secondary ions have already started to contribute significantly to total dose even from the beam entrance to the Bragg peak as shown in figure 4.

3.3. Flat biological dose SOBP of ^{12}C ions

The Bragg peak of a ^{12}C ion beam is so sharp that ripples may appear in the formed SOBP (Grevillot *et al* 2015). Therefore, a ridge filter, also called a ripple filter, is usually used to broaden the Bragg peak in clinical carbon ion therapy. A pseudo ripple filter made of ABS resin (density = 1.04 g cm^{-3}) has been modelled in Monte Carlo simulations of each pristine carbon ion beam to remove the ripples in the later optimized SOBP.

The target value was still set to 3.8 Gy (RBE) in the biological dose optimization procedure to expect a cell survival rate of 10% for H460 cells. In addition to the physical dose and biological dose, RBE, α and β , DSB yield, and cell survival rate of H460 cells from ^{12}C ions with an SOBP ranging from 5 to 10 cm in water are shown in figures 5(A)–(D). The biological dose in the fragmentation tail of ^{12}C beams is higher than for ^4He beams (figure 3(A)) but the biological dose of ^{12}C beams at the entrance is lower. No large data fluctuations (small ripples and spikes) were observed for RBE and α values in the fragmentation of ^{12}C beams as were found with protons and ^4He beams. This improved precision is possibly owing to the relatively high fluence of secondary particles.

The high complexity of the radiation field generated by carbon ions has made the analysis of the biological effect of ^{12}C ion beams more complicated than that for protons and ^4He ions. As shown in figure 5(A), the RBE for ^{12}C beams is much higher than for ^4He and proton beams. Proximal to the SOBP, the RBE varies slowly from 1.4 to 1.9. Within the SOBP, the RBE increases up to 3.9. In the distal edge, the RBE increases up to 4.9 and then decreases. In the fragmentation tail, the RBE first decreases rapidly and then starts to increase slowly with depth, which is different from the continually increasing trend found for the ^4He beams.

Equation (16) in the supplementary material can still be used to explain the biological observations. The RBE variation trend in figure 5(A) is the same as the trend for α and β in figure 5(B). The physical dose continues to drop slowly in the tail and the RBE can be qualitatively analyzed in the edge distal to the Bragg peak and the associated tail knowing that α and β are determined by the energy (or LET) of the ions. The characteristics of both of primary and secondary particles should be considered in analyzing the biological effects. In the distal edge, the decrease of primary beam energy (LET, α and β increase) and the decrease of dose can all result in the increase of the RBE. Later, all of the primary particles stop inside the medium, so only secondary particles can contribute to the dose. Without primary particles, there will not be more secondary ions generated and the fluence of existing secondary ions will continue to decrease. Some low energy recoils may stop as well, so the average energy of recoils may increase (similar to the beam hardening effect), resulting in a decrease of the LET and a decrease of α and β . Later, the secondary recoils continue to lose energy so the LET will start to increase, resulting in an increase

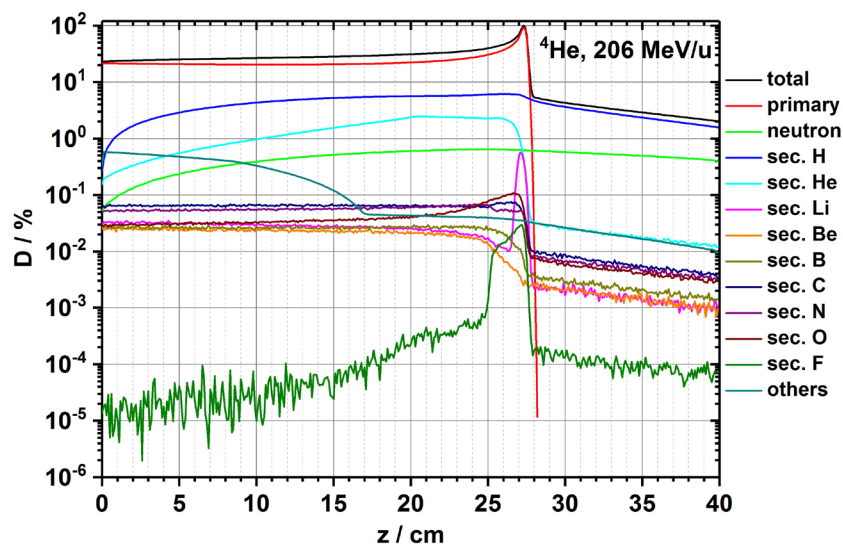


Figure 4. The percent dose contributions from primary and secondary particles for a 206 MeV/u ^4He ion beam in water.

of α and β and an increase of the RBE. The reported variation trend of α along the beam path using the RMF mechanism is consistent with the published work by Inaniwa *et al* (2010) using a modified MKM mechanism for human salivary gland tumor cells (Inaniwa *et al* 2010). The reported RBE values and spatial variation trend are consistent with the previously published data by Frese *et al* (2012) and Kamp *et al* (2015) (Frese *et al* 2012, Kamp *et al* 2015).

For the DSB induction data in figure 5(C), the normalized DSB yield (per Gy per Gbp) increases within the SOBP, but the absolute DSB yield (per Gbp) at a given dose level decreases with depth along the SOBP, which is also different from the constant absolute DSB yield observed in ^4He beams. Although the absolute induced DSB decreases with depth along the SOBP, the frequency of intra-track exchange-type chromosome aberrations increases due to the very high LET at deeper depths. After DNA damage processing, the total lethal DNA lesions may be uniform across the SOBP, so the final cell survival rate is uniform within the SOBP.

The cell survival curve for ^{12}C ions is shown in figure 5(D). In the fragmentation tail, the surviving fraction starts increasing from 0.86 to 0.96 at $z = 15$ cm in water. Compared with proton and ^4He beams, the cell survival in the fragmentation tail of ^{12}C ions is lower because of the relatively higher biological dose mainly contributed by nuclear fragments.

Figure 5(E) shows the beam compositions used to form the ^{12}C SOBP. 38 groups of beam energy from 115.0 to 224.0 MeV/u were used but the data from group #16 with 150.0 MeV/u and group #18 with 154.0 MeV/u are unseen owing to their relatively low contributions. In figure 5(F), the relative difference between the delivered biological dose after the optimization and the prescribed value varies from -1.5% to 1.0% for the whole target region. However, except at the target boundaries, the relative difference is much lower and nearly within $\pm 0.3\%$, showing the high accuracy of the biological dose optimization.

Similar to the study for ^4He ions, Geant4 Monte Carlo simulations were also performed to investigate the dose contributions from primary and secondary particles for a mono-energetic ^{12}C ion beam (400 MeV/u), shown in figure 6. More nuclear interactions are involved between the ^{12}C beam and the medium so the dose contributions from nuclear fragments are very high. Our results also reveal that the main nuclear fragments are protons and ^4He ions (details not shown). The contributions from other secondary particles such as lithium, beryllium, and boron species are also considerable.

3.4. Discussions in describing and reporting the biological effects for clonogenic cell survival

The spatially varied RBE values for different ion beams have been reported above. Some concepts should be reiterated for appropriately describing and reporting the biological effects of particle therapy. One should be cautious in applying these quantities to avoid erroneously extending these results in ways that the data do not support.

First, the RBE for cell survival is defined as the dose ratio when the test radiation and reference radiation result in the same cell surviving fraction for the specified cell type. At different surviving fractions, the RBE values are dose and radiosensitivity dependent. Therefore, the basic requirement for reporting RBE and comparing RBE among different beam qualities is that the same cell surviving fraction criterion must be met (Hall and Giaccia 2012).

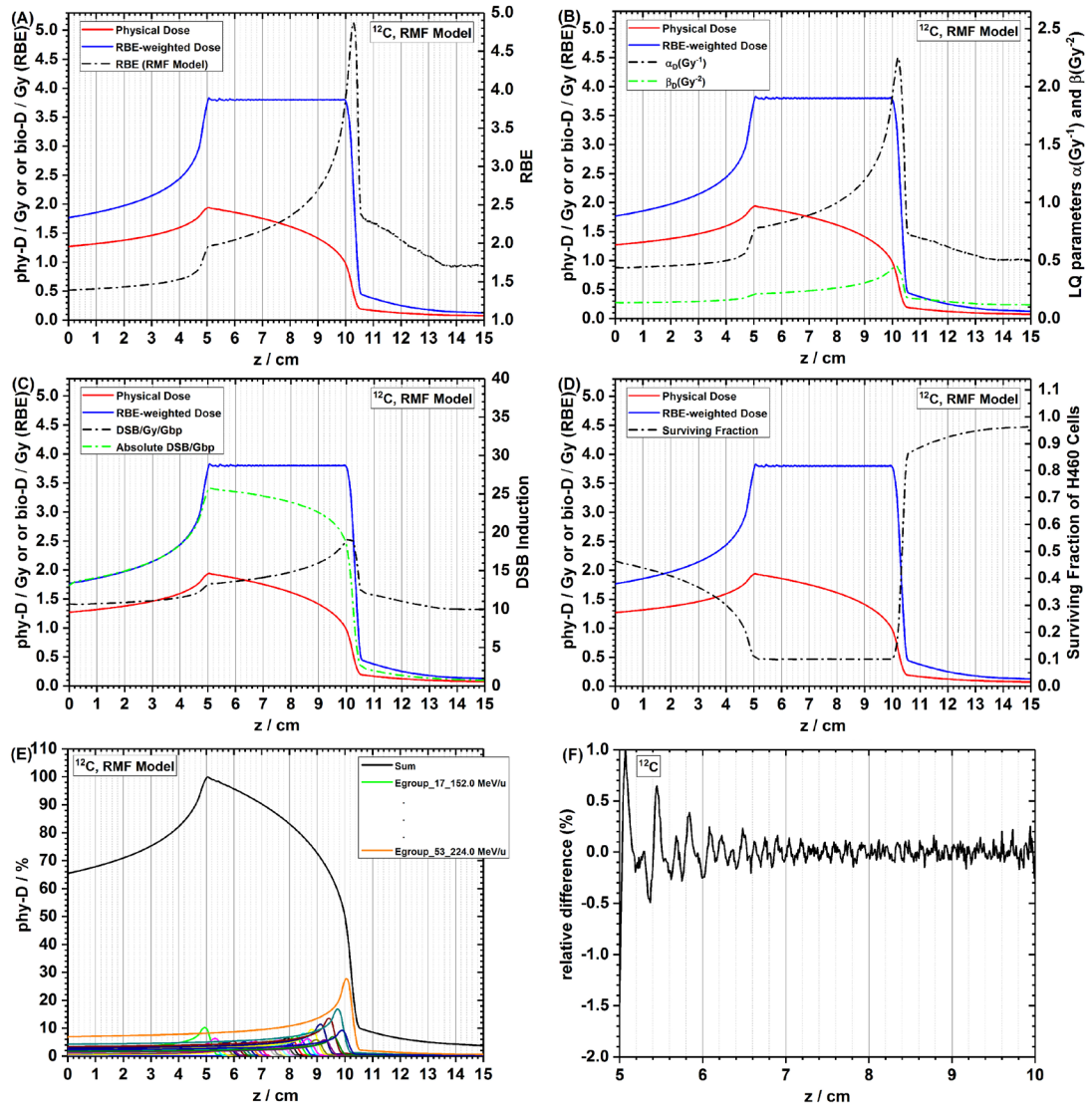


Figure 5. Biological dose optimization results of ^{12}C ion beams. The target region is 5 to 10 cm in water. The target biological dose value is set as 3.8 Gy (RBE). RBE and additional radiobiological parameters are calculated using the RMF model. Cell survival is calculated using the LQ model. In addition to physical dose (phy-D) and biological dose (bio-D) distributions, the following are shown: (A) RBE, (B) the dose-averaged α and β values, (C) the DSB induction with units of DSB/Gy/Gbp and DSB/Gbp at current physical dose level, (D) the surviving fraction of H460 cells. (E) Total physical dose (%) and its constituent weighted dose components. (F) The relative difference between the delivered biological dose after the optimization and the prescribed biological dose within the target prior to the optimization.

Second, the RBE is used to describe the relative level of the biological effect of the test radiation to the reference photons, rather than the absolute level. Therefore, a high RBE at a region does not indicate that the absolute biological effect therein, such as the cell kill, is high as well. For example, in the fragmentation tail of ^4He ions, the RBE is high according to RMF model predictions, but the cell kill effect is low (as described in section 3.2). By contrast, the biological dose, i.e. the RBE-weighted dose to produce the same biological effect as the reference photons, is the appropriate radiobiological quantity to estimate the absolute biological effect. Moreover, an identical biological dose for the same cell line means having the same cell survival rate if the LQ cell survival model is applied.

3.5. Limitations of the current work

Although the dose optimization strategy developed in the current study is very flexible, there are some limitations for our method of generating basic datasets. For example, the microdosimetric quantity y_F is not accurately calculated in Monte Carlo simulations. LET is simply used instead of y_F . This simplification is valid only when the energy of the charged particle is high enough so that it can pass through the target cell without changing the LET along the particle path through the cell (ICRU 1983, Lindborg and Waker 2017). When the particle range becomes comparable to the diameter of the target cell or cell nucleus, this simplification can generate large uncertainties because the particle's LET varies greatly along its path and it may stop inside the target. These effects are especially

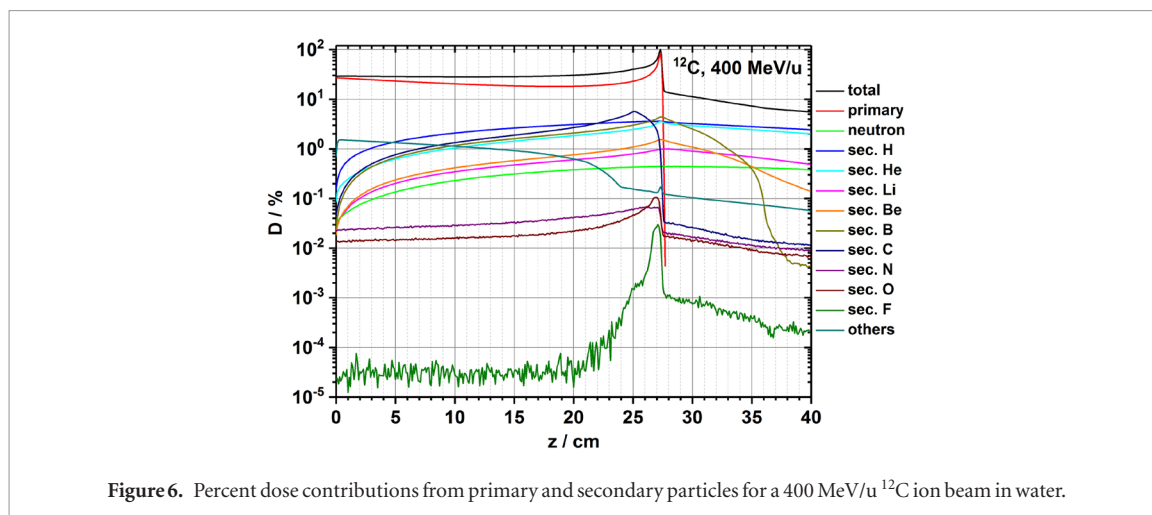


Figure 6. Percent dose contributions from primary and secondary particles for a 400 MeV/u ^{12}C ion beam in water.

important for very low energy particles around the Bragg peak. These calculations of microdosimetric quantities will be refined in our future work to improve the accuracy of calculation results.

Another simplification in the current work is the assumption that lung cancer cells are distributed uniformly in the whole phantom. In practice, outside the target tumor are normal tissues. The biological response of cancer cells and normal cells to radiation can be quite different; therefore, the biological dose calculations for tumor cells and normal cells should be treated distinctly. For complete biological optimization, normal tissue tolerances and responses must also be understood and quantified in the appropriate biological context for effective modelling (Jones 1999). Thus, the tissue heterogeneities in real patients increase the complexity in making bio-IMIT plans. The experimental results of our ongoing studies in normal tissue response using the 3D culture technique will be reported in future. Even for a given cell type, the heterogeneity still exists in the radiobiological response. One practical way to study the impact of heterogeneity in radiosensitivity is to perform a sensitivity analysis of the modelling results over the expected distribution of radiosensitivity, which is currently under investigation by Carlson *et al*.

In addition, only 1D longitudinal data were used in the optimization process in the current study. To extend this work to more complex two- and three-dimensional heterogeneous patient geometry, more accurate dose calculation algorithms should be implemented in the optimization process. Extending our Python based repository to generate full biological dose IMIT optimizations for complex and heterogeneous patient geometries will be one of our next steps.

In addition to the mechanism-based RMF model demonstrated in this study, other biophysical models, e.g. MKM, LEM IV, and a recently developed α and β calculation formalism by Vassiliev *et al* (2017), can also be invoked in the optimization process. The data generation and optimization algorithms for these models will be developed in our future work.

4. Summary and conclusions

It has been demonstrated the feasibility and flexibility of the combined use of Geant4 Monte Carlo simulations and the Python programming language to perform biological dose optimization procedures for different ions using the mechanism-based RMF model for RBE predictions. Some important differences have been observed in biological effects among the three selected ion types, i.e. protons, helium, and carbon ions, which are critical to understand in order to fully achieve biological optimization in particle therapy. For example, for the identical prescribed biological dose level in the target region, carbon ions can deliver the lowest biological dose in the entrance region but can deliver the highest and longest nuclear fragmentation tail. Within the specified 5–10 cm target region in water, the RBE at 10% cell survival rate for H460 cells varies from 1.10 to 1.25 for protons, 1.30 to 1.80 for helium ions, and 1.90 to 3.90 for carbon ions, respectively. One direct application of the current study is that the generated beam delivery strategy can be used in next-step radiobiology experiments using our developed high-throughput strategy (Guan *et al* 2015a) to obtain biological data to further validate the accuracy of the applied RBE calculation model as well as *in vivo* studies using animal models. The experimental results will be reported in future work.

Acknowledgments

This work was supported by National Institutes of Health grants U19 CA021239 and U24 CA180803. The authors would like to thank Dr Robert Stewart from University of Washington for discussing the use of MCDS software.

We thank Dr Geoffrey Ibbott for sharing his knowledge in radiation biology and Erica Goodoff for her editorial assistance.

ORCID iDs

Fada Guan  <https://orcid.org/0000-0001-8477-7391>

References

- Agostinelli S A J et al 2003 Geant4—a simulation toolkit *Nucl. Instrum. Methods Phys. Res. A* **506** 250–303
- Allison J et al 2016 Recent developments in Geant4 *Nucl. Instrum. Methods Phys. Res. A* **835** 186–225
- Alloni D, Campa A, Friedland W, Mariotti L and Ottolenghi A 2013 Integration of Monte Carlo simulations with PFGE experimental data yields constant RBE of 2.3 for DNA double-strand break induction by nitrogen ions between 125 and 225 keV μm^{-1} LET *Radiat. Res.* **179** 690–7
- Berger M J 1995 ESTAR, PSTAR and ASTAR: Computer programs for calculating stopping powers and ranges for electrons, protons and helium ions *Technical Report IAEA-TECDOC-799* (Vienna, Austria: International Atomic Energy Agency) pp 723–39
- Britten R A, Nazaryan V, Davis L K, Klein S B, Nichiporov D, Mendonca M S, Wolanski M, Nie X, George J and Keppel C 2013 Variations in the RBE for cell killing along the depth-dose profile of a modulated proton therapy beam *Radiat. Res.* **179** 21–8
- Brun R and Rademakers F 1997 ROOT—an object oriented data analysis framework *Nucl. Instrum. Methods Phys. Res. A* **389** 81–6
- Butkus M, Stewart R, Chen Z and Carlson D 2018 Double strand break (DSB) complexity and proximity effects within the repair-misrepair fixation (RMF) model for improved predictions of cell survival from heavy ions *Med. Phys.* **45** E532–3
- Carabe-Fernandez A, Dale R G and Jones B 2007 The incorporation of the concept of minimum RBE (RBE min) into the linear-quadratic model and the potential for improved radiobiological analysis of high-LET treatments *Int. J. Radiat. Biol.* **83** 27–39
- Carlson D J, Stewart R D, Semenenko V A and Sandison G A 2008 Combined use of Monte Carlo DNA damage simulations and deterministic repair models to examine putative mechanisms of cell killing *Radiat. Res.* **169** 447–59
- Chaudhary P et al 2014 Relative biological effectiveness variation along monoenergetic and modulated Bragg peaks of a 62 MeV therapeutic proton beam: a preclinical assessment *Int. J. Radiat. Oncol. Biol. Phys.* **90** 27–35
- Chen Y and Ahmad S 2011 Empirical model estimation of relative biological effectiveness for proton beam therapy *Radiat. Protection Dosim.* **149** 116–23
- Dale R G and Jones B 1999 The assessment of RBE effects using the concept of biologically effective dose *Int. J. Radiat. Oncol. Biol. Phys.* **43** 639–45
- Eaton B R, Esiashvili N, Kim S, Weyman E A, Thornton L T, Mazewski C, MacDonald T, Ebb D, MacDonald S M and Tarbell N J 2016 Clinical outcomes among children with standard-risk medulloblastoma treated with proton and photon radiation therapy: a comparison of disease control and overall survival *Int. J. Radiat. Oncol. Biol. Phys.* **94** 133–8
- Elsässer T, Krämer M and Scholz M 2008 Accuracy of the local effect model for the prediction of biologic effects of carbon ion beams *in vitro* and *in vivo* *Int. J. Radiat. Oncol. Biol. Phys.* **71** 866–72
- Elsässer T and Scholz M 2007 Cluster effects within the local effect model *Radiat. Res.* **167** 319–29
- Elsässer T et al 2010 Quantification of the relative biological effectiveness for ion beam radiotherapy: direct experimental comparison of proton and carbon ion beams and a novel approach for treatment planning *Int. J. Radiat. Oncol. Biol. Phys.* **78** 1177–83
- Flanz J and Bortfeld T 2013 Evolution of technology to optimize the delivery of proton therapy: the third generation *Semin. Radiat. Oncol.* **23** 142–8
- Frese M C, Yu V K, Stewart R D and Carlson D J 2012 A mechanism-based approach to predict the relative biological effectiveness of protons and carbon ions in radiation therapy *Int. J. Radiat. Oncol. Biol. Phys.* **83** 442–50
- Friedland W, Jacob P, Bernhardt P, Paretzke H G and Dingfelder M 2003 Simulation of DNA damage after proton irradiation *Radiat. Res.* **159** 401–10
- Friedland W, Jacob P, Paretzke H G and Stork T 1998 Monte Carlo simulation of the production of short DNA fragments by low-linear energy transfer radiation using higher-order DNA models *Radiat. Res.* **150** 170–82
- Furusawa Y, Fukutsu K, Aoki M, Itsukaichi H, Eguchi-Kasai K, Ohara H, Yatagai F, Kanai T and Ando K 2000 Inactivation of aerobic and hypoxic cells from three different cell lines by accelerated ^3He -, ^{12}C - and ^{20}Ne -ion beams *Radiat. Res.* **154** 485–96
- Geng C, Gates D, Bronk L, Ma D and Guan F 2018 Physical parameter optimization scheme for radiobiological studies of charged particle therapy *Phys. Med.* **51** 13–21
- Gillmann C, Lomax A J, Weber D C, Jäkel O and Karger C P 2018 Dose–response curves for MRI-detected radiation-induced temporal lobe reactions in patients after proton and carbon ion therapy: does the same RBE-weighted dose lead to the same biological effect? *Radiother. Oncol.* **128** 109–14
- Grevillot L, Stock M and Vatnitsky S 2015 Evaluation of beam delivery and ripple filter design for non-isocentric proton and carbon ion therapy *Phys. Med. Biol.* **60** 7985–8005
- Guan F, Geng C, Ma D, Bronk L, Kerr M, Li Y, Gates D, Kroger B, Sahoo N and Titt U 2018 RBE model-based biological dose optimization for proton radiobiology studies *Int. J. Part. Ther.* **5** 160–71
- Guan F et al 2015a Spatial mapping of the biologic effectiveness of scanned particle beams: towards biologically optimized particle therapy *Sci. Rep.* **5** 9850
- Guan F et al 2015b Analysis of the track- and dose-averaged LET and LET spectra in proton therapy using the geant4 Monte Carlo code *Med. Phys.* **42** 6234–47
- Hall E J and Giaccia A J 2012 *Radiobiology for the Radiologist* (Philadelphia, PA: Williams & Wilkins)
- Hara Y, Takada Y, Hotta K, Tansho R, Nihei T, Suzuki Y, Nagafuchi K, Kawai R, Tanabe M and Mizutani S 2012 Improvement of spread-out Bragg peak flatness for a carbon-ion beam by the use of a ridge filter with a ripple filter *Phys. Med. Biol.* **57** 1717
- Hawkins R 1996 A microdosimetric-kinetic model of cell death from exposure to ionizing radiation of any LET, with experimental and clinical applications *Int. J. Radiat. Biol.* **69** 739–55
- Hawkins R B 1994 A statistical theory of cell killing by radiation of varying linear energy transfer *Radiat. Res.* **140** 366–74
- Hawkins R B 1998 A microdosimetric-kinetic theory of the dependence of the RBE for cell death on LET *Med. Phys.* **25** 1157–70
- Howard M E, Beltran C, Anderson S, Tseung W C, Sarkaria J N and Herman M G 2017 Investigating dependencies of relative biological effectiveness for proton therapy in cancer cells *Int. J. Part. Ther.* **4** 12–22

- ICRU 1983 *Report 36: Microdosimetry, International Commission on Radiation Units and Measurements* (Bethesda, MD: ICRU)
- ICRU 2007 Prescribing, recording, and reporting proton-beam therapy (ICRU Report 78) *J. ICRU* 7
- Inaniwa T, Furukawa T, Kase Y, Matsufuji N, Toshito T, Matsumoto Y, Furusawa Y and Noda K 2010 Treatment planning for a scanned carbon beam with a modified microdosimetric kinetic model *Phys. Med. Biol.* **55** 6721
- Jones B 1999 Mathematical models of tumour and normal tissue response *Acta Oncol.* **38** 883–93
- Jones B 2014 Patterns of failure after proton therapy in medulloblastoma *Int. J. Radiat. Oncol. Biol. Phys.* **90** 25–6
- Jones B, McMahon S and Prise K 2018 The radiobiology of proton therapy: challenges and opportunities around relative biological effectiveness *Clin. Oncol.* **30** 285–92
- Kamp F, Cabal G, Mairani A, Parodi K, Wilkens JJ and Carlson D J 2015 Fast biological modeling for voxel-based heavy ion treatment planning using the mechanistic repair-misrepair-fixation model and nuclear fragment spectra *Int. J. Radiat. Oncol. Biol. Phys.* **93** 557–68
- Kamp F, Carlson D and Wilkens J 2017 Rapid implementation of the repair-misrepair-fixation (RMF) model facilitating online adaption of radiosensitivity parameters in ion therapy *Phys. Med. Biol.* **62** N285
- Kase Y, Kanai T, Matsufuji N, Furusawa Y, Elsässer T and Scholz M 2007 Biophysical calculation of cell survival probabilities using amorphous track structure models for heavy-ion irradiation *Phys. Med. Biol.* **53** 37
- Krämer M, Jäkel O, Haberer T, Kraft G, Scharadt D and Weber U 2000 Treatment planning for heavy-ion radiotherapy: physical beam model and dose optimization *Phys. Med. Biol.* **45** 3299
- Krämer M and Scholz M 2000 Treatment planning for heavy-ion radiotherapy: calculation and optimization of biologically effective dose *Phys. Med. Biol.* **45** 3319–30
- Lindborg L and Waker A 2017 *Microdosimetry: Experimental Methods and Applications* (Boca Raton, FL: CRC Press)
- Mailhot Vega R B, Kim J, Bussière M, Hattangadi J, Hollander A, Michalski J, Tarbell N J, Yock T and MacDonald S M 2013 Cost effectiveness of proton therapy compared with photon therapy in the management of pediatric medulloblastoma *Cancer* **119** 4299–307
- Mairani A et al 2016 Biologically optimized helium ion plans: calculation approach and its *in vitro* validation *Phys. Med. Biol.* **61** 4283–99
- McNamara A L, Schuemann J and Paganetti H 2015 A phenomenological relative biological effectiveness (RBE) model for proton therapy based on all published *in vitro* cell survival data *Phys. Med. Biol.* **60** 8399–416
- Mohan R, Peeler C R, Guan F, Bronk L, Cao W and Grosshans D R 2017 Radiobiological issues in proton therapy *Acta Oncol.* **56** 1367–73
- Nikjoo H, O'Neill P, Terrissol M and Goodhead D 1994 Modelling of radiation-induced DNA damage: the early physical and chemical event *Int. J. Radiat. Biol.* **66** 453–7
- Nikjoo H, O'Neill P, Terrissol M and Goodhead D 1999 Quantitative modelling of DNA damage using Monte Carlo track structure method *Radiat. Environ. Biophys.* **38** 31–8
- Paganetti H 2014 Relative biological effectiveness (RBE) values for proton beam therapy. Variations as a function of biological endpoint, dose, and linear energy transfer *Phys. Med. Biol.* **59** R419–72
- Paganetti H 2018 Proton relative biological effectiveness—uncertainties and opportunities *Int. J. Part. Ther.* **5** 2–14
- Paganetti H, Niemierko A, Ancukiewicz M, Gerweck L E, Goitein M, Loeffler J S and Suit H D 2002 Relative biological effectiveness (RBE) values for proton beam therapy *Int. J. Radiat. Oncol. Biol. Phys.* **53** 407–21
- Particle Therapy Co-Operative Group 2017 Particle therapy facilities in clinical operation (<https://www.ptcog.ch/index.php/facilities-in-operation>) (Accessed: 18 December 2017)
- Patel D, Bronk L, Guan F, Peeler C R, Brons S, Dokic I, Abdollahi A, Rittmüller C, Jäkel O and Grosshans D 2017 Optimization of Monte Carlo particle transport parameters and validation of a novel high throughput experimental setup to measure the biological effects of particle beams *Med. Phys.* **44** 6061–73
- Polster L, Schuemann J, Rinaldi I, Burigo L, McNamara A L, Stewart R D, Attali A, Carlson D J, Sato T and Méndez J R 2015 Extension of TOPAS for the simulation of proton radiation effects considering molecular and cellular endpoints *Phys. Med. Biol.* **60** 5053
- Qin N, Shen C, Tsai M-Y, Pinto M, Tian Z, Dedes G, Pompos A, Jiang S B, Parodi K and Jia X 2018 Full Monte Carlo-based biologic treatment plan optimization system for intensity modulated carbon ion therapy on graphics processing unit *Int. J. Radiat. Oncol. Biol. Phys.* **100** 235–43
- Sakama M, Kanai T, Kase Y, Yusa K, Tashiro M, Torikai K, Shimada H, Yamada S, Ohno T and Nakano T 2012 Design of ridge filters for spread-out Bragg peaks with Monte Carlo simulation in carbon ion therapy *Phys. Med. Biol.* **57** 6615–33
- Scholz M, Kellerer A M, Kraft-Weyrather W and Kraft G 1997 Computation of cell survival in heavy ion beams for therapy. The model and its approximation *Radiat. Environ. Biophys.* **36** 59–66
- Sigmund P, Schinner A and Paul H 2009 Errata and addenda for ICRU report 73, stopping of ions heavier than helium *ICRU J.* **5**
- Stewart R D, Carlson D J, Butkus M P, Hawkins R, Friedrich T and Scholz M 2018 A comparison of mechanism-inspired models for particle relative biological effectiveness (RBE) *Med. Phys.* **45** e925–e952
- Stewart R D, Yu V K, Georgakilas A G, Koumenis C, Park J H and Carlson D J 2011 Effects of radiation quality and oxygen on clustered DNA lesions and cell death *Radiat. Res.* **176** 587–602
- Stock M, Georg P, Mayer R, Böhlen T T and Vatnitsky S 2015 Development of clinical programs for carbon ion beam therapy at MedAustron *Int. J. Part. Ther.* **2** 474–7
- Tilly N, Johansson J, Isacson U, Medin J, Blomquist E, Grusell E and Glimelius B 2005 The influence of RBE variations in a clinical proton treatment plan for a hypopharynx cancer *Phys. Med. Biol.* **50** 2765
- Vassiliev O N, Grosshans D R and Mohan R 2017 A new formalism for modelling parameters α and β of the linear–quadratic model of cell survival for hadron therapy *Phys. Med. Biol.* **62** 8041
- Wedenberg M, Lind B K and Hårdemark B 2013 A model for the relative biological effectiveness of protons: the tissue specific parameter α/β of photons is a predictor for the sensitivity to LET changes *Acta Oncol.* **52** 580–8
- Wilkens JJ and Oelfke U 2004 A phenomenological model for the relative biological effectiveness in therapeutic proton beams *Phys. Med. Biol.* **49** 2811–25
- Yock T I et al 2016 Long-term toxic effects of proton radiotherapy for paediatric medulloblastoma: a phase 2 single-arm study *Lancet Oncol.* **17** 287–98